

## Research Article

# Modeling the Compression Behavior of Dredged Sandy Clays Considering the Effect of Initial Water Contents and Sand Fractions

Jian Yang,<sup>1</sup> Yiwen Zeng,<sup>1</sup> Xian Sun,<sup>2</sup> and Jiaying Weng<sup>3</sup> 

<sup>1</sup>Key Lab of Ministry of Education for Geomechanics and Embankment Engineering, Hohai University, Nanjing 210098, China

<sup>2</sup>Changjiang Water Resources Commission, River and Lake Protection and Construction Operation Safety Center, Wuhan 430000, China

<sup>3</sup>Jiangsu Water Source Company Ltd. of the Eastern Route of the South-to-North Water Diversion Project, Nanjing 210000, China

Correspondence should be addressed to Jiaying Weng; [wengjiayingseu@163.com](mailto:wengjiayingseu@163.com)

Received 11 August 2023; Revised 24 August 2023; Accepted 4 September 2023; Published 25 September 2023

Academic Editor: Jiangyu Wu

Copyright © 2023 Jian Yang et al. This is an open access article distributed under the Creative Commons Attribution License, which permits unrestricted use, distribution, and reproduction in any medium, provided the original work is properly cited.

Dredged sandy clays are widely utilized as fill material in geotechnical projects, and their compressibility is crucial to the engineering design. It is well recognized that the compression behavior of dredged sandy clays is significantly affected by the initial water content and sand fraction. Besides, these two physical properties are usually spatially dependent due to the process of hydraulic filling. In this study, an effective compression model is formulated based on the equivalent void ratio concept. The compression curve of pure clays is first established as a reference, which depends on the initial void ratio and liquid limit. Then, the effect of sand fraction has been incorporated by directly implementing the equivalent void ratio into the reference curve. A structural variable is introduced to describe the evolving intergranular structure with coarse content and stress level. Only one additional structural parameter is required, and it can be readily calibrated by one traditional compression test. Validation shows that the model is effective in reproducing the compression behavior of dredged sandy clays with a wide range of initial water content and sand fraction. The proposed equation can provide a reasonable reference for establishing the hardening law and the corresponding general constitutive model of dredged sandy clays.

## 1. Introduction

Hydraulic fill method has been well adopted in land reclamation and waterway dredging engineering [1–5]. The natural depositions are mixed with water and pumped from river/sea bed, leading to a high porosity of dredged sandy clays, which results in poor mechanical properties (e.g., low stiffness and shear resistance). In this case, a drainage treatment is required in engineering practices to reduce the water content before this type of soil can be reused as construction material in airports and harbors [6, 7]. To this end, a practical estimation on the compressibility of dredged sandy clays is required for the engineering design of those geostructures [1–3, 6–8].

The in situ investigation shows that there is usually a spatial variability in water content and gradation in dredged

sandy clays due to the process of hydraulic transportation. In detail, with the increasing distance from dredge pump, the water content gradually decreases while the sand fraction gradually increases [9, 10]. Previous studies based on laboratory work have collectively reported that the compression behavior of dredged sandy clays is significantly affected by the initial state and sand fraction [10–19]. The compressibility decreases with the decrease of initial water content and increases with the decrease of sand fraction. Two different types of compression model have been proposed for describing this behavior: (1) empirical or semiempirical models based on the database of experimental tests and phenomenological approaches [1–3, 11, 20, 21], for example, Hong et al. [1] and their coworkers proposed a series of empirical models to reproduce the intrinsic compression line of reconstituted soils with various initial void ratios; and (2)

theoretical models within the framework of mixture theory [4, 22] and equivalent void ratio concept [23, 24]. For instance, a structural variable has been introduced by Shi and Yin [4] to describe the evolution of intergranular structure of dredged sandy clays with various sand fractions. However, the effect of initial water content is not incorporated.

In this work, a simple yet practical model is proposed to evaluate the effect of initial water content and sand fraction on the compression behavior of dredged sandy clays. A reference model is first formulated for pure clays. Then, the equivalent void ratio concept is further adopted to describe the evolving soil structure and the corresponding sand fraction effect. Validation reveals that the proposed model can well reproduce the test results and possesses a higher accuracy than empirical method.

## 2. Compression Curve for Pure Clays Incorporating the Effect of Initial Water Content

In situ investigations on dredging project have indicated that the sand fraction of dredged sandy clays is usually below the transitional value (i.e., a certain value of clay/sand content which distinguishes the dominated structure in sand–clay mixture) [11, 12, 17–19, 23], leading to a fine-dominated structure (i.e., sand particles are suspended in the soft clay matrix and play a secondary role in the loading transmission). In this case, the compression behavior of dredged sandy clays is mainly controlled by the soft clay matrix [4, 16, 24, 25]. Therefore, the intrinsic compression curve of pure clays can be adopted as a reference for evaluating the effect of initial water content and sand fraction.

As noted by Hong et al. [1], the reconstituted clay with high initial water content shows a semielastic compression behavior within the remold yield stress ( $\sigma'_{cy}$ ), which is analogous to the behavior of structured soils [10, 26]. Besides, the compression line beyond  $\sigma'_{cy}$  can be well captured by a linear relationship in double logarithmic plot [1, 19]. Note that the effective stress of dredged sandy clays during preloading process is usually beyond the remold yield stress [1–3, 19, 21]. Therefore, the deformation behavior in semielastic range can be deemed insignificant. A linear compression line of pure clays is defined to capture the compression behavior of the pure clay matrix [27]:

$$\ln(v_c) = \ln(1 + e_{1000}) - \frac{\ln(1 + e_{1000}) - \ln(1 + e_{c0})}{\ln(\sigma'_{cy}) - \ln(\sigma'_r)} \ln\left(\frac{\sigma'_c}{\sigma'_r}\right), \quad (1)$$

where  $v_c$  and  $\sigma'_c$  are the specific volume ( $v_c = 1 + e_c$ ) and effective stress of pure clays, respectively; and  $e_{c0}$  represents the initial void ratio of the pure clays. Note that the volumetric deformation of reconstituted soils within  $\sigma'_{cy}$  is assumed to be negligible due to the extremely high bulk modules [19, 28]; and  $\sigma'_r = 1,000$  kPa is employed as a reference stress and  $e_{1000}$  denotes the corresponding void ratio [29].

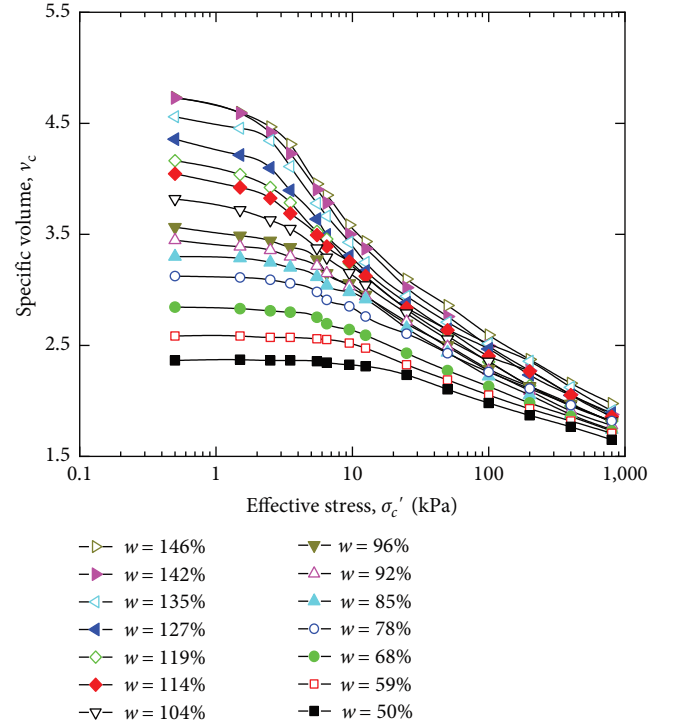


FIGURE 1: Typical compression curves of reconstituted Lianyungang clay (data from Hong et al. [1]).

**2.1. Effect of Initial Water Content.** Typical compression behavior of reconstituted clays with different initial water contents is presented in Figure 1 (data from Hong et al. [1]). It can be seen that for a given effective stress, the void ratio and compressibility both decrease with a decreasing initial water content. Besides, the semielastic range narrows down continually as the initial void ratio increases. Evidently, the reference void ratio ( $e_{1000}$ ) and remolded yield stress ( $\sigma'_{cy}$ ) vary with initial water content. According to laboratory investigation in previous research, those two physical variables are directly related to  $e_{c0}$  and the void ratio at liquid limit ( $e_{cL}$ ) [1–3, 21, 30, 31]. By performing multiple-regression analysis on the database compiled from the literature [1–4, 22] (detailed soil properties are given in Table 1), Equations (2) and (3) are formulated to determine  $e_{1000}$  and  $\sigma'_{cy}$ . Note that there might be an absence of the compression data at 1,000 kPa for some of the experimental results from the literature. In this case, the data values are extrapolated based on the measured compression curve.

$$e_{1000} = 0.05e_{c0} + 0.88e_{cL}, \quad (2)$$

$$\sigma'_{cy} = 3.21 \frac{e_{c0}}{e_{cL}} - 2.41. \quad (3)$$

The comparison between the model predictions and test data is presented in Figure 2. It can be seen that the errors between calculated results and experimental data are both within 10%, which show a good performance of the proposed equations. Substitution of Equations (2) and (3) into

TABLE 1: Details of the physical properties of soils.

Soils	$\rho_c$ (g/cm <sup>3</sup> )	$w_L$ (%)	$w$ (%)	References
Lianyungang clay	2.71	73.7	50.0, 59.0, 68.0, 78.0, 85.0, 92.0, 104.0, 114.0, 119.0, 127.0, 135.0, 142.0, and 146.0	Hong et al. [1]
Baimahu clay	2.65	90.6	64.0, 72.0, 83.0, 91.0, 101.0, 111.0, 119.0, 126.0, 137.0, 143.0, 153.0, 163.0, 174.0, and 180.0	
Kemen clay	2.67	61.1	43.0, 48.0, 57.0, 62.0, 66.0, 72.0, 80.0, 87.0, 91.0, 99.0, 106.0, 110.0, 116.0, and 122.0	
Huaian clay	2.70	100.0	80.6, 100.2, 119.5, 139.9, 159.7, and 179.6	Zeng et al. [2]
	2.72	86.0	88.8 and 132.9	
	2.70	72.7	79.0 and 109.0	
	2.70	59.7	92.9	
	2.70	46.5	71.3	
	2.69	77.1	77.7 and 112.7	
	2.69	66.7	100.9	
	2.69	57.4	89.3	
	2.72	72.3	74.6 and 136.5	
	2.69	60.5	61.5	
Wenzhou clay	2.70	64.9	64.0	
	2.68	64.8	65.1	
	2.67	60.8	58.6	
	2.68	62.1	52.5	
	2.72	63.0	96.6 and 125.0	
Nanjing clay	2.71	46.7	46.2 and 76.3	
	2.70	43.8	42.2	
	2.72	52.0	46.8	
Taizhou clay	2.63	69.5	69.0	
	2.66	60.1	42.7 and 84.6	
Fuzhou clay	2.72	69.3	86.2	Zeng et al. [3]
	2.66	67.0	67.2	
Hong Kong marine clay	2.68	62.4	67.9, 74.5, 86.9, and 99.5	Shi and Yin [4]
Bentonite	2.70	524.0	744.0 and 885.0	Shi et al. [22]

$\rho_c$  = the density of clay particles;  $w_L$  = the liquid limit of the soil;  $w$  = the initial water content of the soil.

Equation (1) yields a complete compression curve for pure clays with various initial water contents and liquid limits:

$$\ln(v_c) = \ln(1 + 0.05e_{c0} + 0.88e_{cL}) - \frac{\ln(1 + 0.05e_{c0} + 0.88e_{cL}) - \ln(1 + e_{c0})}{\ln[3.21(e_{c0}/e_{cL})^{-2.41}] - \ln(\sigma'_r)} \ln\left(\frac{\sigma'_r}{\sigma'_r}\right). \quad (4)$$

The compression data of four different reconstituted clays [1, 4] are used to further evaluate the accuracy of the proposed compression curve. The physical properties of soils used for comparison are summarized in Table 1. The predicted compression curves are compared with experimental data in Figure 3. The model works well in describing the compressibility of reconstituted clays with different initial water contents, and is consistent with the experimental data (especially after the remolded yield stress). Thus, the proposed model in Equation (4) could provide a good

reference for estimating the compressibility of dredged sandy clays with different clay fractions.

### 3. Intrinsic Compression Curve of Dredged Sandy Clays with Different Initial Water Contents and Sand Fractions (Model 1)

**3.1. Effect of Sand Fraction.** The coarse aggregates (e.g., sand and gravel) usually disperse in soft clay matrix of dredged sandy clays with a fine-dominated structure, leading to a decrease of void space and compressibility [4, 19, 32–34]. In this case, the relative content of clay matrix and coarse particles should be considered when evaluating the compression behavior of dredged sandy clays. First, the initial void ratio of dredged sandy clays with different sand fractions can be expressed according to its definition:

$$e_0 = \frac{(1 - \psi)\rho_s}{\psi\rho_s + (1 - \psi)\rho_s} e_{c0}, \quad (5)$$

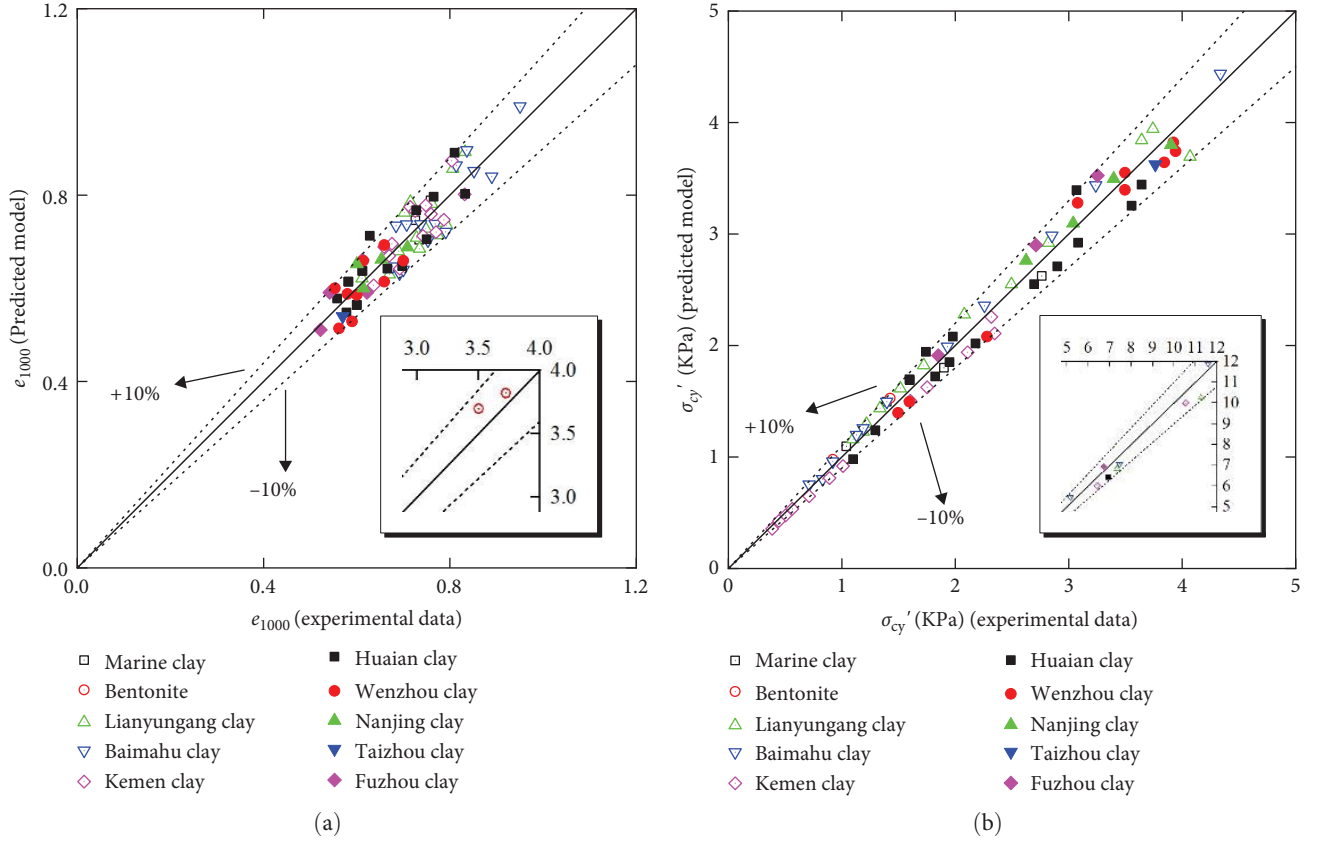


FIGURE 2: Comparison of model indices calculated by measurements and equations for reconstituted clays [1–4, 22]: (a) reference void ratio for pure clays ( $e_{1000}$ ); and (b) remolded yield stress for pure clays ( $\sigma'_{cy}$ ).

where  $\psi$  is the dry mass fraction of sand (coarse) particles;  $\rho_s$  and  $\rho_c$  denote the particle density of coarse and clay, respectively.

Since the sand particles in dredged sandy clays cannot be compressed, the volume change under stress compression is caused by the clay–water system related to the water content. The liquid limit, as an indicator of water contents, is closely related to the components of the dredged sandy clays. When the water content of a saturated soil reaches the liquid limit, the sand particles are suspended within the clay–water system. At this point, the percentage of sand fraction relative to the sum of sand and clay fractions reaches a critical value. When the water content reaches the liquid limit, there are two states of the dredged sandy clays: (1) when the sand fraction is less than the critical percentage, the sand particles remain suspended in the clay–water system and do not come into contact with each other; and (2) the sand particles come into contact with each other when the sand fraction is greater than the critical percentage, increasing the soil’s resistance to deformation and reducing deformation, thereby allowing the soil to retain more water.

Previous studies on diverse clay–sand/gravel mixtures have demonstrated that the water holding capacity of dredged sandy clays is primarily governed by the clay particles [35–37]. Consequently, the liquid limit of dredged sandy clays exhibits a downward trend with an increase in sand fraction, establishing an inverse correlation between sand

fraction and the liquid limit of mixtures. To this end, the void ratio of dredged sandy clays at liquid limit ( $e_L$ ) is correlated with the sand fraction, and a linear relationship between  $e_L$  and  $\psi$  (when  $\psi$  is below 75%) has been reported by previous researchers [38]:

$$e_L = (1 - \psi)e_{cL}. \quad (6)$$

Equation (6) is employed to describe the effect of coarse inclusions on the compressibility of dredged sandy clays. Note that the “75%” is an approximate value of the transition coarse content  $\psi_{th}$  of dredged sandy clays, which relies on the nature of soil particles (e.g., mineralogy and particle size distribution), and may vary within a narrow range. For simplicity,  $\psi_{th} = 75\%$  is adopted herein, which is consistent with the experimental results of most dredged sandy clays [38, 39].

Replacing  $e_{c0}$  and  $e_{cL}$  in Equation (4) by  $e_0$  and  $e_L$  in Equations (5) and (6), one obtains the intrinsic compression curve of dredged sandy clays with various initial void ratios and sand fractions.

$$\ln(v) = \ln(1 + 0.05e_0 + 0.88e_L) - \frac{\ln(1 + 0.05e_0 + 0.88e_L) - \ln(1 + e_0)}{\ln[3.21(e_0/e_L)^{-2.41}] - \ln(\sigma'_r)} \ln\left(\frac{\sigma'}{\sigma'_r}\right), \quad (7)$$

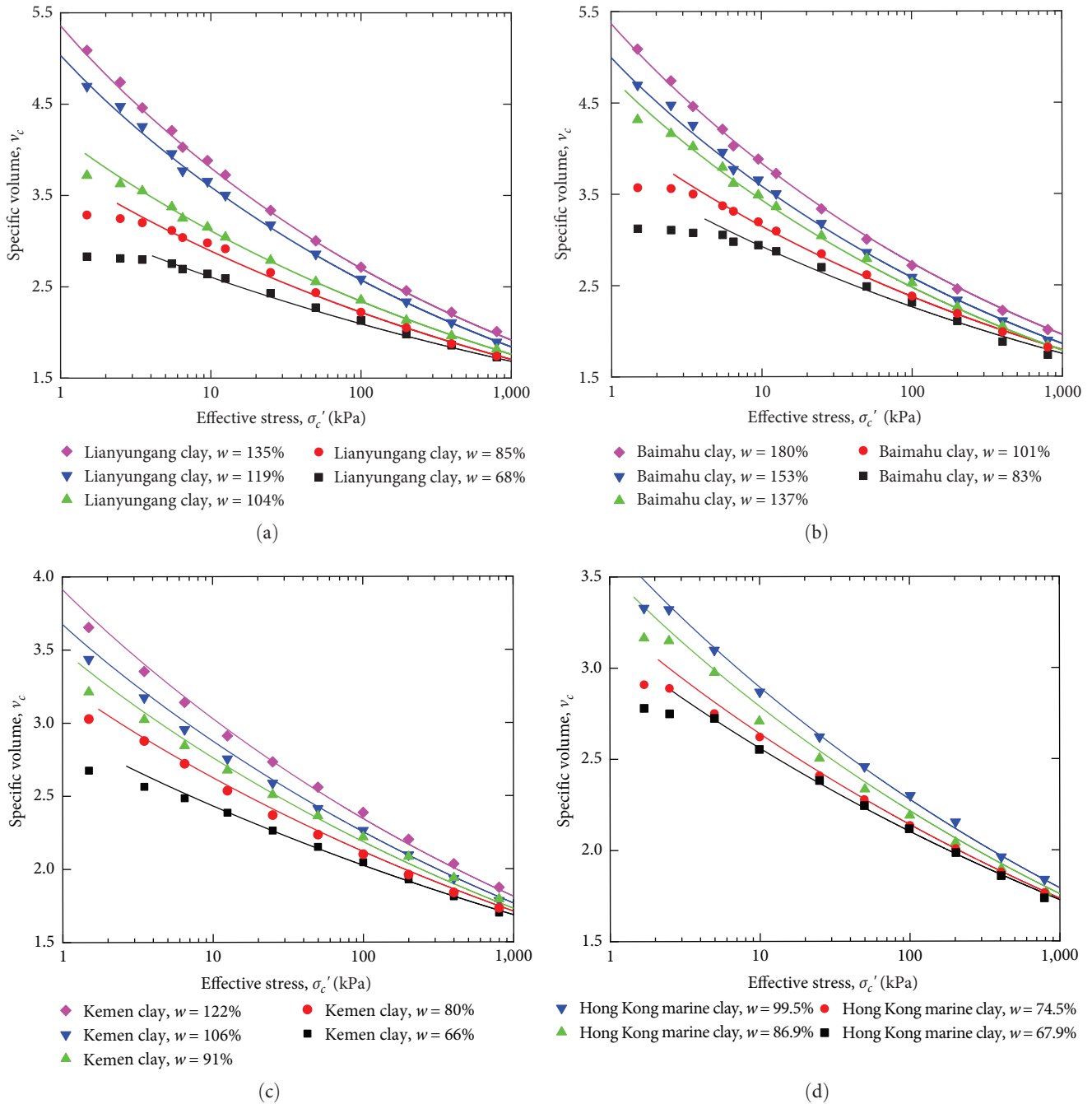


FIGURE 3: Comparison of measured data and predicted compression curves for reconstituted clays [1, 4]: (a) Lianyungang clay; (b) Baimahu clay; (c) Kemen clay; and (d) Hong Kong marine clay.

where  $v$  and  $\sigma'$  are the specific volume ( $v = 1 + e$ ) and effective vertical stress of the dredged sandy clays, respectively. Equation (7) is termed as Model 1 herein to avoid confusion.

3.2. Validation for Model 1. Model 1 is verified by the compression test data of two different clay-sand/gravel mixtures: (1) sand-marine clay mixtures [4]; and (2) sand-bentonite mixtures [22]. The particle densities of the coarse particle in

these two mixtures are 2.63 and 2.69, respectively, with corresponding minimum void ratios at maximum packing of 0.601 and 0.55, respectively. A summary of the basic physical properties of those mixtures and the values of model parameter required for this study are listed in Table 2.

The predicted compression curves (lines) and corresponding test data of sand-marine clay mixtures and sand-bentonite mixtures (dots) are presented in Figures 4

TABLE 2: Physical properties and values of model parameters for mixtures from the literature.

Host clay	$\rho_c$ and $\rho_s$ (g/cm <sup>3</sup> )	$e_{\max}$ and $e_{\min}$	$w$ (%)	$\psi$ (%)	$\delta$	References
Hong Kong marine clay	2.68/2.63	0.945/0.601	67.9, 74.5, 86.9, and 99.5	0, 20, 40, and 60	0.24	Shi and Yin [4]
Bentonite	2.70/2.69	0.890/0.550	744.0 885.0	0, 50, 65, and 75 0, 65, and 75	0.15	Shi et al. [22]

$e_{\max}$  and  $e_{\min}$  = the maximum and minimum void ratios of coarse aggregates, respectively.

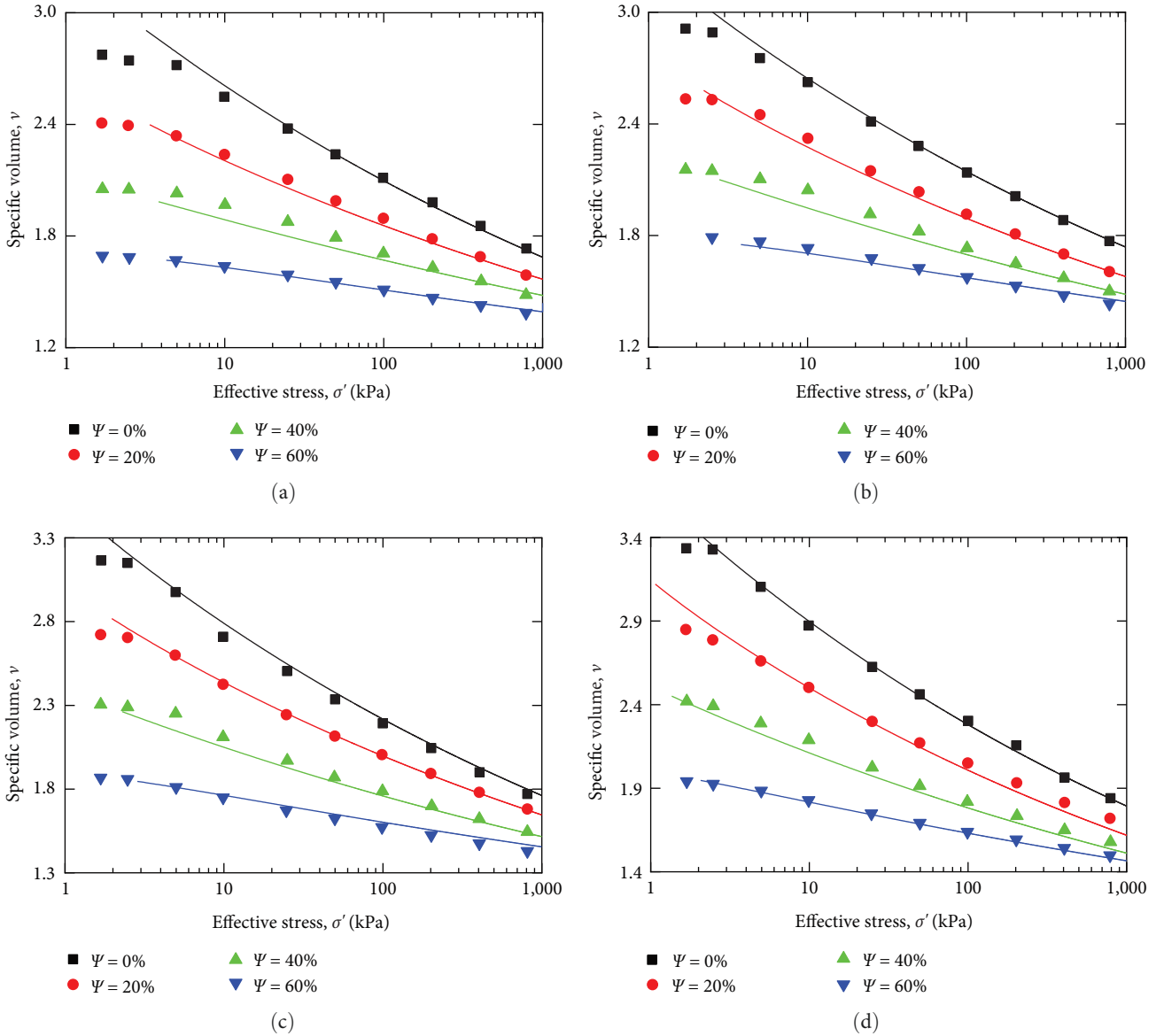


FIGURE 4: Comparison of measured data and predicted compression curves for the sand–marine clay mixtures from Shi and Yin [4] (Model 1): (a)  $w = 67.9\%$ ; (b)  $w = 74.5\%$ ; (c)  $w = 86.9\%$ ; and (d)  $w = 99.5\%$ .

and 5, respectively. It is seen that the main features of the compression behavior can be captured by Model 1: the compression curve shifts upward, and the compressibility of the dredged sandy clay rises with an increase in initial water content. Besides, the overall stiffness of the dredged sandy clays increases with rising sand fraction, revealing a reinforcing effect of sand particles on the compressibility of dredged sandy clays.

#### 4. Compression Curve of Dredged Sandy Clays Based on Equivalent Void Ratio (Model 2)

4.1. *Equivalent Void Ratio for Dredged Sandy Clays.* As mentioned above, dredged sandy clays usually process a certain amount of coarse aggregates, leading to a clay–sand/gravel mixture. Previous studies on this type of soils have shown that the mechanical properties are well affected by the



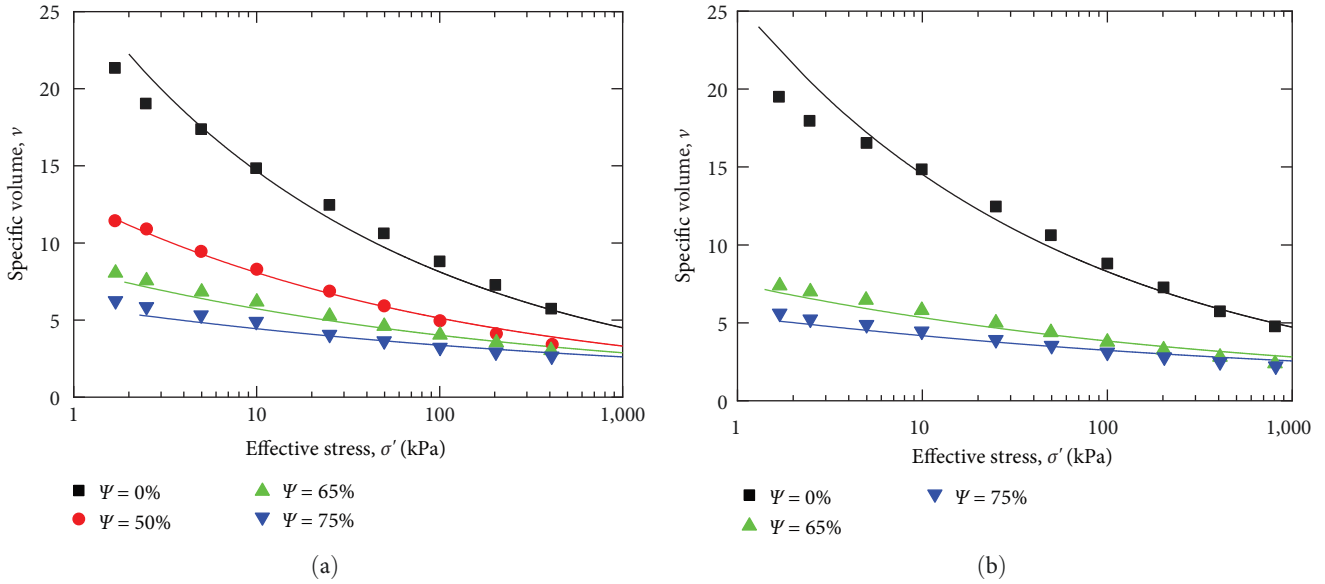


FIGURE 5: Comparison of measured data and predicted compression curves for the sand–bentonite mixtures from Shi et al. [22] (Model 1): (a)  $w = 744\%$ ; and (b)  $w = 855\%$ .

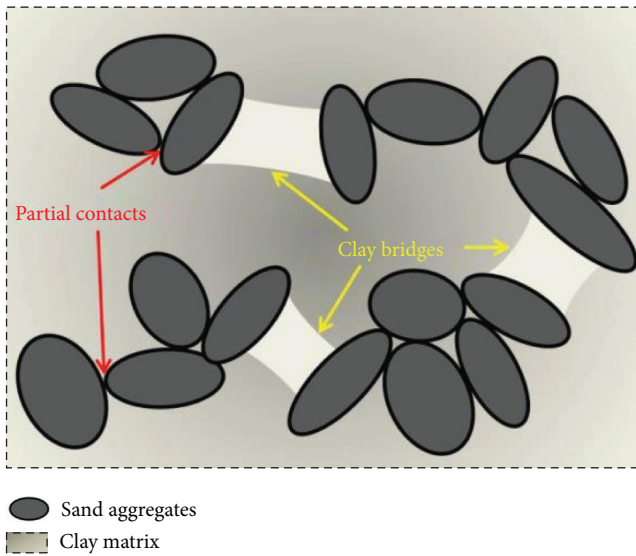


FIGURE 6: Schematic diagram of the internal structure of dredged sandy clays.

evolving intergranular structure with sand fraction and stress level [4, 19, 23–25, 33, 40, 41]. The mechanisms governing this effect can be interpreted in the following two aspects: (1) incompressible sand particles occupy the void space in the clay matrix, leading to a decrease in compressibility; and (2) the compacted “clay bridge” and partial contacts between sand particles result in a stress concentration, which reduces the local stress in the deformable clay matrix, and leads to an increase in overall stiffness [42].

A schematic diagram of the internal structure of dredged sandy clays is presented in Figure 6. Although the validation in last section shows a relatively satisfactory performance of Model 1, it is limited in describing the evolution of

intergranular structure of dredged sandy clays with varying sand fractions. To this end, a novel compression model based on the equivalent concept is proposed in the sequel for a better description of effect of sand fraction on the compressibility of dredged sandy clays.

Previous studies on clay–sand/gravel mixtures indicate that the equivalent void ratio is effective in capturing the evolving structure as well as the reinforcement effect of coarse aggregates [19, 23, 24, 43, 44]. For example, Zeng et al. [24] proposed an equivalent compression curve for clay–sand/gravel mixtures, which is proved to be effective in normalizing the compression lines of clay–sand/gravel mixtures with various sand fractions, overcoming the shortcomings of the semi-empirical method (Model 1) used above. The equivalent void ratio concept was initially proposed by Thevanayagam and Mohan [43] for particle mixtures. Due to the high particle size ratio between sand and clay particles in dredged sandy clays, the original version cannot effectively reflect the contribution of increased sand fraction to the overall mechanical properties of the soil, therefore, the void ratio in the compression law of pure clays [27] has been directly replaced by the modified equivalent void ratio  $e_{eq}$  [19]:

$$e_{eq} = \frac{e}{1 - \psi + \kappa \cdot \psi}, \quad (8)$$

where  $\kappa$  is a structure variable responsible for the reinforcing effect of sand particles on the compressibility of dredged sandy clays, and it is positively correlated with the sand fraction. As noted by Shi et al. [19], the following requirements should be satisfied for the clay–sand mixtures: (1) the effect of sand inclusions is negligible ( $\kappa = 0$ ) when the sand fraction approaches to zero; and (2) the mixture is nearly incompressible as the sand particle reaches its densest packing state, resulting in an infinite value of the structural

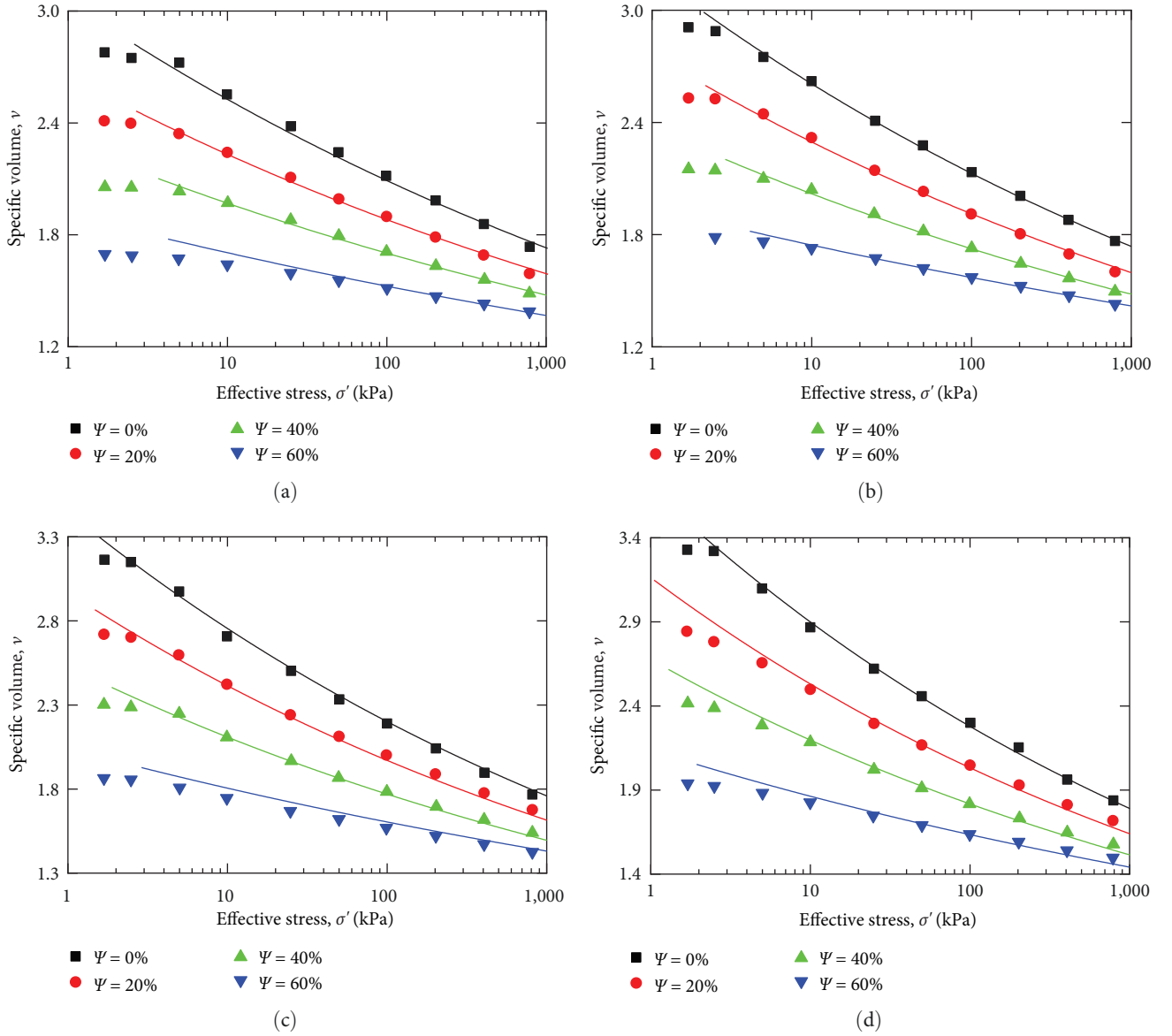


FIGURE 7: Comparison of measured data and predicted compression curves for the sand–marine clay mixtures from Shi and Yin [4] (Model 2): (a)  $w = 67.9\%$ ; (b)  $w = 74.5\%$ ; (c)  $w = 86.9\%$ ; and (d)  $w = 99.5\%$ .

variable ( $\kappa \rightarrow \infty$ ). Considering the requirements mentioned above, Equation (9) is introduced to capture the evolution of the intergranular structure of dredged sandy clays.

$$\kappa = \left[ \frac{1}{\varphi - (1 - \varphi)e_{\min}} \right]^{\delta} - 1, \quad (9)$$

where  $e_{\min}$  represents the minimum void ratio of sand (coarse) aggregates;  $\delta$  is a structural parameter controlling the sensitivity of the structure variable  $\kappa$  to the sand fraction [24], and  $\varphi$  is the volume fraction of clay matrix. The structural parameter  $\delta$  controls the evolution of interaggregates structure with sand fraction and stress level. It only depends on the basic physical properties of the sand particle (e.g., particle shape, roughness, and particle-size distribution), and can be calibrated from one oedometer test on dredged

sandy clay with a relatively high sand fraction [19, 24, 34]. Compared to the mass fraction, the volume fraction of sand  $\varphi$  (a state-dependent variable) can evaluate the evolution of interparticle structure under different sand fractions and stress levels [19, 24]:

$$\varphi = \frac{\psi \rho_c}{(1 + e)[\psi \rho_c + (1 - \psi)\rho_s]}. \quad (10)$$

Refer to the work from Zeng et al. [24], the concept of equivalent void ratio is further adopted in this study to capture the effect of sand fraction on the compression behavior of dredged sandy clays with various initial water contents. Combining Equations (4) and (8), a new compression curve for dredged sandy clays base on the equivalent void ratio (Model 2) is obtained:



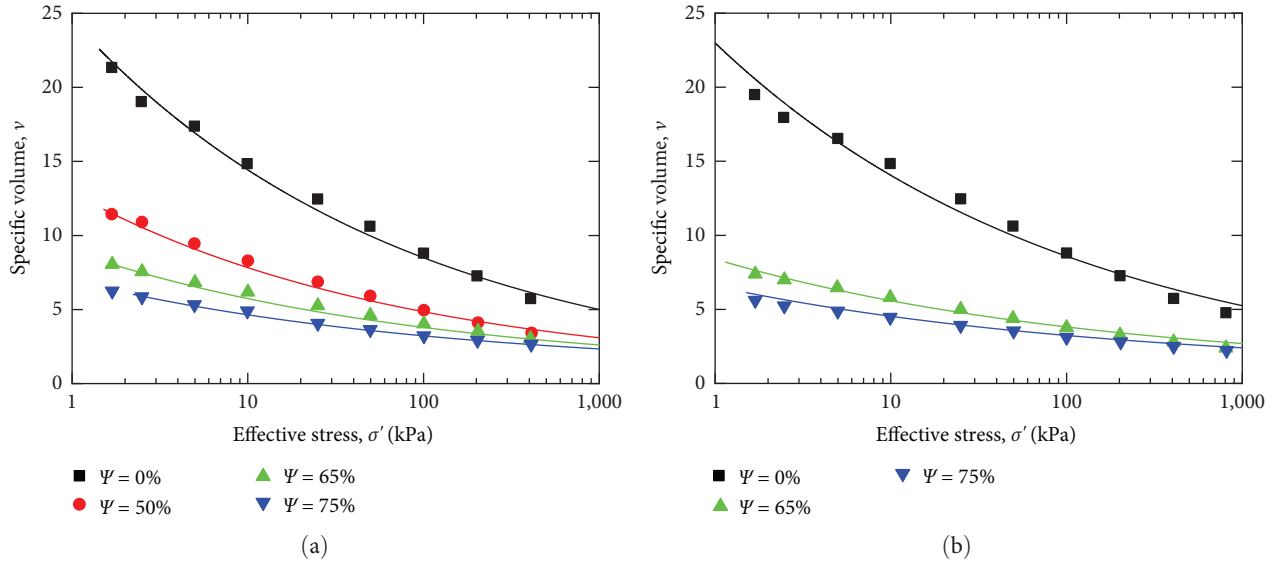


FIGURE 8: Comparison of measured data and predicted compression curves for the sand–bentonite mixtures from Shi et al. [22] (Model 2): (a)  $w = 744\%$ ; and (b)  $w = 855\%$ .

$$v = 1 + (1 - \psi + \kappa \cdot \psi) \cdot \left\{ \exp \left[ \ln(1 + 0.05e_0 + 0.88e_L) - \frac{\ln \left( \frac{1+0.05e_0+0.88e_L}{1+e_0} \right)}{\ln \left[ \frac{3.21(e_0/e_L)^{-2.41}}{\sigma_r'} \right]} \ln \left( \frac{\sigma'}{\sigma_r'} \right) \right] - 1 \right\}. \quad (11)$$

Note that the sand aggregates may be crushed under high-stress level, which results in particle rearrangement and affects the compressibility. However, for dredged sandy clay with clay fraction beyond the “transition fine content”, the sand particles are surrounded by soft clay, which provides a confining pressure and protects the coarse aggregates from breakage [4]. In this case, the effect of particle breakage on the compressibility of dredged sandy clay is negligible and not be incorporated into the models.

**4.2. Validation for Model 2.** Compared with Model 1, an additional structure parameter  $\delta$  is required in Model 2 to evaluate the evolution of intergranular structure of dredged sandy clays with different sand fractions. The structure parameter is dependent on the basic physical properties of the coarse aggregates in dredged sandy clays (e.g., gradation, roughness, and particle shape), and it can be determined from one oedometer test on the dredged sandy clays with a relative high sand fraction (50%–70%).

The experimental data introduced in last section are also utilized for the validation of Model 2, and the calibrated structural parameter are given in Table 2. The predicted compression results (lines) and test data (dots) are plotted in Figures 7 and 8. It can be observed that after introducing the equivalent void ratio to consider the internal structural evolution of dredged sandy clays, it is still found that the compression curve moves upward and the overall initial void ratio increases with the increase of initial water content, leading to an increase in the compressibility of dredged sandy clays. As the clay fraction increases, the compression curve becomes higher, and the overall compressibility

increases. The results indicate that, compared with the semi-empirical method (Model 1), Model 2 is more effective in estimating the compressibility of dredged sandy clays with different sand fractions, and reveals that the structure parameter is independent on the sand fractions.

**4.3. Comparison between Model 1 and Model 2.** As above-mentioned, both of the Model 1 and Model 2 can capture the main features of the compression behavior of the dredged sandy clays, for example, the effect of initial water content, sand fraction and nature of clay particles (liquid limit). To further evaluate the capacity of the proposed two models, a comparison between the test data and the predicted results of Model 1 and Model 2 are summarized in Figures 9(a) and 9(b), respectively. It is seen that the maximum error of Model 1 is 10%, revealing a promising application prospect in engineering projects. Besides, after introducing the equivalent void ratio concept to capture the internal structure evolution of dredged sandy clays, the prediction effect of Model 2 is further improved, and the maximum error is further reduced to 5%. Model 2 indicates a good capacity of the equivalent void ratio in describing the evolution of internal structure of dredged sandy clays, and it might provide a reference for modeling the general elastic–plastic behavior of dredged sandy clays.

The semiempirical method (Model 1) can capture the influence of clay fraction under different initial water content conditions with reasonable accuracy without introducing an additional parameter, which basically meets the engineering requirements. Nevertheless, the incorporation of one single model parameter to Model 2 can be achieved with

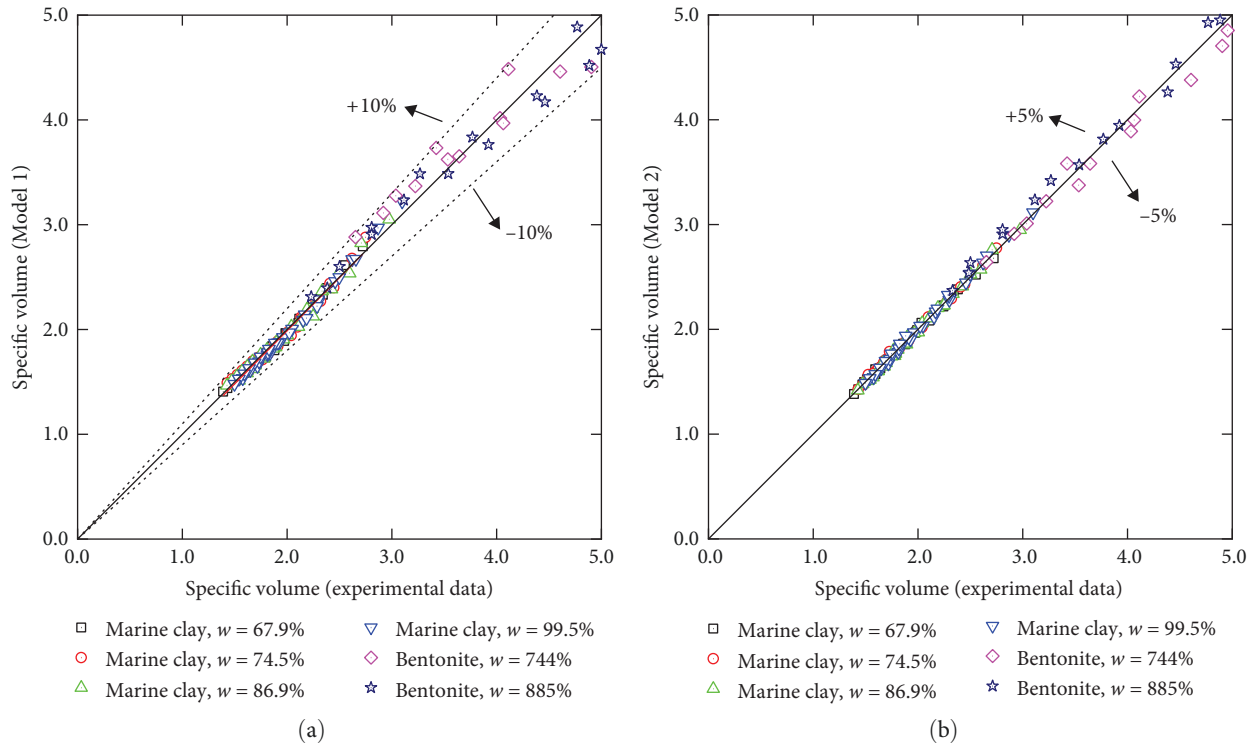


FIGURE 9: Comparisons between compression model predicted and oedometer test data: (a) Model 1; and (b) Model 2.

straightforward adjustment, without excessively complicating the method. Simultaneously, it captures the impact of the evolution of interparticle structure on its mechanical properties, rendering it more universally applicable.

## 5. Conclusions

The water content and gradation of dredged sandy clays are usually spatial-dependent variables, which results a variation of the compressibility of this geomaterial. A compression model has been proposed for dredged sandy clays based on the equivalent void ratio concept, which considers the combined effect of initial water content and sand fraction. It is further validated by the experimental data from literature. The following summaries can be drawn:

- (1) A reference compression line is first established for pure dredged clays by performing a multiple regression analysis on the available data base. Validation shows that the effect of initial water content of the compressibility of dredged clays can be well captured by the proposed model. Besides, a semiempirical method (Model 1) is proposed for dredged sandy clays. This is done by incorporating the linear relationship between the liquid limit and sand fraction into the reference line.
- (2) A structural variable is further introduced to describe the evolution of interparticle structure of dredge sandy clays with rising sand fraction and stress level. Furthermore, the revised equivalent void ratio of

sand–clay mixture is implemented into the reference compression line, and a novel compression model (Model 2) is proposed within the framework of equivalent concept.

- (3) Only one model parameter is required for the proposed Model 2, and it can be readily calibrated from one single compression test. Comparison between the test data and predicted results indicates that the Model 2 is simple yet practical in capturing the compression behavior of dredged sandy clays with a wide range of initial water contents and sand fractions.

## Data Availability

The data supporting the current study are given in the article.

## Conflicts of Interest

The authors declare that there is no conflict of interest regarding the publication of this paper.

## Acknowledgments

The authors gratefully acknowledge the financial support received from the Jiangsu Funding Program for Excellent Postdoctoral Talent, number 2022ZB815, the Jiangsu South to North Water Diversion Technology R&D Project, number JSNSBD202205, and the China Postdoctoral Science Foundation, number 2023M731816.

## References

- [1] Z.-S. Hong, J. Yin, and Y.-J. Cui, "Compression behaviour of reconstituted soils at high initial water contents," *Géotechnique*, vol. 60, no. 9, pp. 691–700, 2010.
- [2] L.-L. Zeng, Z.-S. Hong, and Y.-J. Cui, "Determining the virgin compression lines of reconstituted clays at different initial water contents," *Canadian Geotechnical Journal*, vol. 52, no. 9, pp. 1408–1415, 2015.
- [3] L.-L. Zeng, Z.-S. Hong, and Y.-F. Gao, "Practical estimation of compression behaviour of dredged clays with three physical parameters," *Engineering Geology*, vol. 217, pp. 102–109, 2017.
- [4] X. S. Shi and J. Yin, "Experimental and theoretical investigation on the compression behavior of sand–marine clay mixtures within homogenization framework," *Computers and Geotechnics*, vol. 90, pp. 14–26, 2017.
- [5] D.-Y. Tan, J.-H. Yin, W.-Q. Feng, Z.-H. Zhu, J.-Q. Qin, and W.-B. Chen, "New simple method for calculating impact force on flexible barrier considering partial muddy debris flow passing through," *Journal of Geotechnical and Geoenvironmental Engineering*, vol. 145, no. 9, p. 04019051, 2019.
- [6] J. Chu, S. W. Yan, and H. Yang, "Soil improvement by the vacuum preloading method for an oil storage station," *Géotechnique*, vol. 50, no. 6, pp. 625–632, 2000.
- [7] L. Nguyen and B. Fatahi, "Behaviour of clay treated with cement & fibre while capturing cementation degradation and fibre failure—C3F Model," *International Journal of Plasticity*, vol. 81, pp. 168–195, 2016.
- [8] R. J. Chenari, B. Fatahi, A. Ghorbani, and M. N. Alamoti, "Evaluation of strength properties of cement stabilized sand mixed with EPS beads and fly ash," *Geomechanics and Engineering*, vol. 14, pp. 533–544, 2018.
- [9] G.-Z. Xu, Y.-F. Gao, Z.-S. Hong, and J.-W. Ding, "Sedimentation behavior of four dredged slurries in China," *Marine Georesources & Geotechnology*, vol. 30, no. 2, pp. 143–156, 2012.
- [10] X. Bian, Z.-F. Wang, G.-Q. Ding, and Y.-P. Cao, "Compressibility of cemented dredged clay at high water content with super-absorbent polymer," *Engineering Geology*, vol. 208, pp. 198–205, 2016.
- [11] J.-H. Yin, "Properties and behaviour of Hong Kong marine deposits with different clay contents," *Canadian Geotechnical Journal*, vol. 36, no. 6, pp. 1085–1095, 1999.
- [12] A. Khalili, D. Wijewickreme, and G. W. Wilson, "Mechanical response of highly gap-graded mixtures of waste rock and tailings. Part I: Monotonic shear response," *Canadian Geotechnical Journal*, vol. 47, no. 5, pp. 552–565, 2010.
- [13] M. D. Liu, Z. Zhuang, and S. Horpibulsuk, "Estimation of the compression behaviour of reconstituted clays," *Engineering Geology*, vol. 167, pp. 84–94, 2013.
- [14] F. Tong and J.-H. Yin, "Experimental and constitutive modeling of relaxation behaviors of three clayey soils," *Journal of Geotechnical and Geoenvironmental Engineering*, vol. 139, no. 11, pp. 1973–1981, 2013.
- [15] T. Y. Elkady, A. A. Shaker, and A. W. Dhowain, "Shear strengths and volume changes of sand–attapulgitic clay mixtures," *Bulletin of Engineering Geology and the Environment*, vol. 74, no. 2, pp. 595–609, 2015.
- [16] L. Zuo and Béatrice A. Baudet, "Determination of the transitional fines content of sand–non plastic fines mixtures," *Soils and Foundations*, vol. 55, no. 1, pp. 213–219, 2015.
- [17] S. D. Silva, "Three runway system project, contract 3206: main reclamation works," p. 7076481, *Rep. for ZHECC-CCCC-CDC joint venture*, vol. R00, 2016.
- [18] D.-S. Xu, M. Huang, and Y. Zhou, "One-dimensional compression behavior of calcareous sand and marine clay mixtures," *International Journal of Geomechanics*, vol. 20, no. 9, p. 04020137, 2020.
- [19] X. S. Shi, Y. Gao, and J. Ding, "Estimation of the compression behavior of sandy clay considering sand fraction effect based on equivalent void ratio concept," *Engineering Geology*, vol. 280, p. 105930, 2021.
- [20] H. J. Pincus, N. S. Pandian, T. S. Nagaraj, and P. S. R. N. Raju, "Permeability and compressibility behavior of bentonite–sand/soil mixes," *Geotechnical Testing Journal*, vol. 18, no. 1, pp. 86–93, 1995.
- [21] L.-L. Zeng, Z.-S. Hong, and Y.-J. Cui, "United void index for normalizing virgin compression of reconstituted clays," *Canadian Geotechnical Journal*, vol. 57, no. 10, pp. 1497–1507, 2020.
- [22] X. S. Shi, J. Yin, W. Feng, and W. Chen, "Creep coefficient of binary sand–bentonite mixtures in oedometer testing using mixture theory," *International Journal of Geomechanics*, vol. 18, no. 12, 2018.
- [23] X. S. Shi and J. Zhao, "Practical estimation of compression behavior of clayey/silty sands using equivalent void-ratio concept," *Journal of Geotechnical and Geoenvironmental Engineering*, vol. 146, no. 6, p. 04020046, 2020.
- [24] Y. Zeng, X. Shi, W. Chen, and W. Feng, "Equivalent compression curve for clay–sand mixtures using equivalent void-ratio concept," *International Journal of Geomechanics*, vol. 23, no. 2, p. 06022039, 2023.
- [25] M. M. Monkul and G. Ozden, "Compressional behavior of clayey sand and transition fines content," *Engineering Geology*, vol. 89, no. 3–4, pp. 195–205, 2007.
- [26] Z.-S. Hong, L.-L. Zeng, Y.-J. Cui, Y.-Q. Cai, and C. Lin, "Compression behaviour of natural and reconstituted clays," *Géotechnique*, vol. 62, no. 4, pp. 291–301, 2012.
- [27] R. Butterfield, "A natural compression law for soils (an advance on  $e-\log p'$ )," *Géotechnique*, vol. 29, no. 4, pp. 469–480, 1979.
- [28] X. S. Shi, J. Nie, J. Zhao, and Y. Gao, "A homogenization equation for the small strain stiffness of gap-graded granular materials," *Computers and Geotechnics*, vol. 121, p. 103440, 2020.
- [29] J. B. Burland, "On the compressibility and shear strength of natural clays," *Géotechnique*, vol. 40, no. 3, pp. 329–378, 1990.
- [30] Z. Hong, "Void ratio-suction behavior of remolded Ariake clay," *Geotechnical Testing Journal*, vol. 30, no. 3, pp. 234–239, 2006.
- [31] X. S. Shi and I. Herle, "Modeling the compression behavior of remolded clay mixtures," *Computers and Geotechnics*, vol. 80, pp. 215–225, 2016.
- [32] G. V. Kumar, *Some aspects of the mechanical behavior of mixtures of kaolin and coarse sand*, University of Glasgow, 1996.
- [33] M. K. Jafari and A. Shafiee, "Mechanical behavior of compacted composite clays," *Canadian Geotechnical Journal*, vol. 41, no. 6, pp. 1152–1167, 2004.
- [34] X. S. Shi, J. Zhao, and Y. Gao, "A homogenization-based state-dependent model for gap-graded granular materials with fine-dominated structure," *International Journal for Numerical and*

- Analytical Methods in Geomechanics*, vol. 45, no. 8, pp. 1007–1028, 2021.
- [35] H. J. Pincus, T.-S. Tan, T.-C. Goh, G. P. Karunaratne, and S.-L. Lee, “Shear strength of very soft clay–sand mixtures,” *Geotechnical Testing Journal*, vol. 17, no. 1, pp. 27–34, 1994.
- [36] K. Yin, A.-L. Fauchille, E. Di Filippo, P. Kotronis, and G. Sciarra, “A review of sand–clay mixture and soil–structure interface direct shear test,” *Geotechnics*, vol. 1, no. 2, pp. 260–306, 2021.
- [37] G. Wang, X. Bian, Y.-J. Wang, Y.-J. Cui, and L.-L. Zeng, “Effect of organic matter content on Atterberg limits and undrained shear strength of river sediment,” *Marine Georesources & Geotechnology*, vol. 40, no. 9, pp. 1060–1072, 2022.
- [38] E. Polidori, “Relationship between the Atterberg limits and clay content,” *Soils and Foundations*, vol. 47, no. 5, pp. 887–896, 2007.
- [39] A. F. Cabalar and W. S. Mustafa, “Fall cone tests on clay–sand mixtures,” *Engineering Geology*, vol. 192, pp. 154–165, 2015.
- [40] Z.-Y. Yin, H.-W. Huang, and P.-Y. Hicher, “Elastoplastic modeling of sand–silt mixtures,” *Soils and Foundations*, vol. 56, no. 3, pp. 520–532, 2016.
- [41] Z. Xia, R.-P. Chen, and X. Kang, “Laboratory characterization and modelling of the thermal–mechanical properties of binary soil mixtures,” *Soils and Foundations*, vol. 59, no. 6, pp. 2167–2179, 2019.
- [42] X. S. Shi, K. Liu, and J. Yin, “Effect of initial density, particle shape, and confining stress on the critical state behavior of weathered gap-graded granular soils,” *Journal of Geotechnical and Geoenvironmental Engineering*, vol. 147, no. 2, p. 04020160, 2021.
- [43] S. Thevanayagam and S. Mohan, “Intergranular state variables and stress–strain behaviour of silty sands,” *Géotechnique*, vol. 50, no. 1, pp. 1–23, 2000.
- [44] S. Thevanayagam, T. Shenthan, S. Mohan, and J. Liang, “Undrained fragility of clean sands, silty sands, and sandy silts,” *Journal of Geotechnical and Geoenvironmental Engineering*, vol. 128, no. 10, pp. 849–859, 2002.